EasyChair Preprint

№ 11208

From Reduced- to Full-Scale Validation of a Numerical Model of Air Entry in a Penstock Pipe During Valve Closing

William Benguigui, Antoine Archer and Helene Pichon

October 31, 2023

FROM REDUCED- TO FULL-SCALE VALIDATION OF A NUMERICAL MODEL OF AIR ENTRY IN A PENSTOCK PIPE DURING SAFETY VALVE CLOSING

W. Benguigui[1,2], A. Archer[1], H. Pichon[3]

Corresponding author: william.benguigui@edf.fr
[1] EDF R&D, Fluid Mechanic for Energy and Environment department, 6 quai Watier 78400 Chatou
[2] IMSIA UMR EDF/CNRS/CEA/ENSTA Paristech 9219, 7 boulevard Gaspard Monge 91120 Palaiseau, France
[3] EDF CIH, Centre d'Ingénierie Hydraulique, 4 All. du Lac de Tignes, 73290 La Motte-Servolex

KEY WORDS

Two-phase flow, numerical modeling, CFD, reduced scale experiment, penstock pipe

ABSTRACT

In penstock pipes, upstream of hydropower stations, a safety valve is located at the top in order to cut the flow rate before the downward slope if necessary. During its closing, the pressure downstream reduces whereas the upstream one remains constant. To avoid low pressures in the penstock pipe, air-venting valves are present and open when the pressure inside the pipe is lower than outside. Once opened, the air from the atmosphere flows into the penstock pipe and counters the pressure decrease. The correct design of air entry systems is of primary interest for hydraulic engineering. The present work is focused on the numerical simulation with neptune_cfd of air entry in a penstock pipe during the safety valve closing. To close or open valves, the CFD model uses a discrete forcing method (Immersed Boundary) to allow solid motion without any need for dynamic re-meshing. For the air-venting valve, its motion depends directly on the pressure forces on its two sides (the atmosphere outside, the penstock pressure inside). The two-phase air-water flow is modeled with an Eulerian-Eulerian approach with a multi-regime model solving large gas structures and modeling bubbles. A dedicated reduced-scale closed-loop experiment is used to characterize the flow in terms of pattern and to record pressure evolution in the pipe. The numerical model is validated for different flow rates and for different number of air-venting valves (1 to 3 with different diameters). Moreover, operating condition data are used to validate the model at full-scale. The numerical model is in a satisfactory agreement with measurements and show its ability to increase our knowledge on the phenomenon of air entry in such configuration.

1. INTRODUCTION

Ensuring safe operation of hydropower is of primary interest for hydraulic engineering. In penstock pipes (see Figure 1), upstream of hydropower stations, a safety valve is located at the top in order to cut the flow rate if necessary (in the valve house in Figure 2).

Figure 1 Picture of penstock pipes.

Due to the high flow rates, its design must comply high civil engineering loads. Moreover, during its closing, the pressure downstream reduces whereas the upstream one remains almost constant, related to the amount of water in the reservoir. To avoid low pressures in the penstock pipe, air-venting valves are present downstream the safety valve and open when the pressure inside the pipe is lower than the atmospheric pressure outside. Once opened, the air from the atmosphere flows into the penstock pipe and counters the pressure decrease. Therefore, the correct design of air entry systems is of primary interest for hydraulic engineering [1,2]. The dynamic of the two-phase flow during safety valve closing is complex and requires to be studied in order to increase our knowledge for the design of air venting systems. In fact, it is necessary to have a connection between air outside and inside the penstock pipe, thus the air intake has to be sufficient to create a inside/outside air connection to counter pressure decrease. However, having larger air venting valves is not always possible since it might affect the integrity of the pipe.

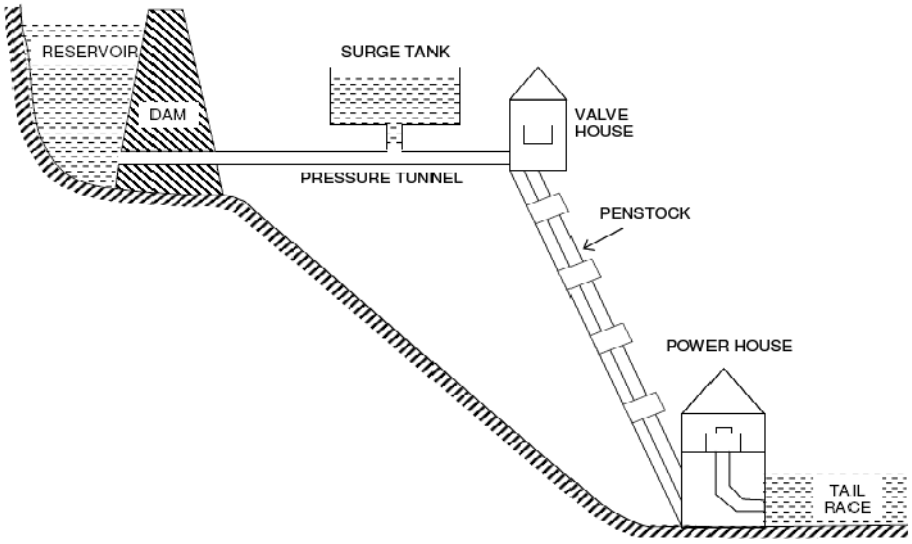

Figure 2 Schematic Arrangement of a Hydro Electric Power Plant

The present work is focused on the numerical simulation of air entry in a penstock pipe during the safety valve closing. To close or open valves, the CFD model uses a discrete forcing method (Immersed Boundary) to allow solid motion without any need for dynamic re-meshing. The motion of the safety valve is imposed by the user. For the air-venting valve, its motion depends directly on the pressure forces on its two sides (the atmosphere outside, the penstock pressure inside). An on/off approach is used, meaning there are two possible positions “open” or “closed”. The two-phase air-

water flow is modeled with an Eulerian-Eulerian approach with a multi-regime model solving large gas structures and modeling dispersed bubbles. A single gas field is used and depending on the gas/liquid fractions and from their gradient, transition laws are able to choose the right (dispersed or Large Interface) interfacial momentum transfer term.
In order to validate the present numerical model, a dedicated reduced-scale closed-loop experiment is used to characterize the flow's pattern and pressure evolution in the pipe.
The numerical model is validated for different flow rates and for different number of air-venting valves (1 to 3 with different diameters). Moreover, operating condition data are used to validate the model at full-scale with gravitational entrainment of water in the penstock pipe (which was not present in the experiment).
First, the numerical model is described from the two-phase flow modeling to the modeling strategy. Then, the reduced scale experiment is described, and the associated numerical validation is presented. Finally, some results based on full-scale operating condition are presented.

2. NUMERICAL MODELING

To simulate the air intake in a penstock pipe, a two-phase numerical solver and a way to represent valve closing/opening are necessary and described below. Then, the numerical setup is presented.

2.1 Two-phase flow numerical modeling

neptune_cfd is a code dedicated to multiphase flows and based on the two-fluid approach [3]. It is a finite-volume code with a collocated arrangement for all variables. The data structure is totally face-based, which allows for the use of cells of arbitrary shape when building the mesh. Using a pressure correction approach [4], it simulates multiphase flows by solving a set of three balance equations for each field (i.e., mass, momentum, and energy balance equations). These balance equations are deduced from the volumetric averaging of local instantaneous balance equations where the k-phase volumetric fraction is written as $\alpha_k \in [0, 1]$. In multiphase flows, one property of the k-phase volumetric fractions is:

$$\sum_{k=1}^{N} \alpha_k = 1 \tag{1}$$

with N being the number of fluid phases included in the fluid domain. Fields can represent different kinds of multiphase flows. The present work is focused on liquid-gas flows only and restricted to adiabatic cases, simplifying the system to the mass and momentum balance equations for each phase k:

$$\frac{\partial(\alpha_k \rho_k)}{\partial t} + \vec{\nabla} \cdot \left(\alpha_k \rho_k \overrightarrow{U_k}\right) = 0 \tag{2}$$

$$\frac{\partial\left(\alpha_k \rho_k \overrightarrow{U_k}\right)}{\partial t} + \vec{\nabla} \cdot \left(\alpha_k \rho_k \overrightarrow{U_k U_k}\right) = -\alpha_k \vec{\nabla} P + \alpha_k \rho_k \vec{g} + \vec{\nabla} \cdot \bar{\bar{\tau}}_k + \sum_{p=1\, p\neq k}^{N} \overrightarrow{M}_{p\to k} \tag{3}$$

where α_k, ρ_k, $\overrightarrow{U_k}$, $\bar{\bar{\tau}}_k$, P, $\vec{g}$, and $\overrightarrow{M}_{p\to k}$ are the volume fraction, the density, the velocity vector and Reynolds-stress tensor of phase k (including also the contribution as a result of fluid viscosity, even in the laminar case), the pressure, the acceleration of gravity, and the momentum transfer from phase p to the phase k, respectively. Note that for air-water flows, the energy transfers between phases can be neglected and the energy balance conservation equation will not be discussed here.

Depending on the two-phase flow structures—that is, large and deformed or small and spherical bubbles or free surface—a dedicated model was used to predict accurately the interfacial momentum transfers of each phase, through the term $\overrightarrow{M}_{p\to k}$ in Eq. 3. For free-surface flows, the large interface model (LIM) is used [5]. A dedicated interfacial friction is consequently applied to both phases with the term $\overrightarrow{M}_{p\to k}$. Whereas for dispersed flow, dedicated dispersed bubble interfacial momentum transfer terms are used for drag, lift or added-mass. In the present work, when large gas structures, free surface or dispersed bubbles are present, an innovative hybrid model is used for the air phase [6,7]. With a single gas field, it is possible to take into account whether dispersed bubbly flow or free surface based on transition law (depending on void gradient) between the dispersed approach and the LIM.
The present algorithm is compressible to allow variation of density (as a function of pressure based on a perfect gas assumption). The compressibility is only applied to the air phase.

2.2 An Immersed Boundary Method to track valve motion

To represent the valves and their motions, a kind of immersed boundary method is used. The aim of discrete forcing methods is to represent solids with a dedicated phase and to strictly ensure the conservation laws at the close vicinity of the fluid-structure interface. The idea is to reshape the cells crossed by the fluid-solid interface and to build specific schemes inside them to discreetly rebuild walls. A recognition function is therefore required to determine the solid location on the cells. The main advantage of these methods lies in the non-explicit representation of the structure, so that, it is possible to perform calculations on complex solid geometries using cartesian or hexahedral meshes. The major challenge of these methods is to reconstruct the interface properties. In the present method, the whole domain is considered in the framework of a porous medium approach, where a time and space dependent fraction, called porosity, is 0 in the solid and 1 in the fluid. The fluid-structure interface is consequently represented with a porosity between 0 and 1; thus Eq 1 becomes:

$$\sum_{k=1}^{N} \alpha_k = \varepsilon \tag{4}$$

with ε the time and space dependent porosity. There is no mass transfer between solid and fluids. Here, the solid motion is tracked thanks to the porosity evolution in a Lagrangian framework. To take into account the solid motion and the presence of an interface in cut-cells, the porosity has to be convected and the momentum balance equations are formulated differently. Based on dedicated geometric parameters, the wall is reconstructed based on interpolations. For low values of porosity, clippings are used to avoid numerical issues. Then, the different two-phase flow numerical models are consequently adapted. This fluid-structure interface tracking method is called time and space-dependent porosity method, further details can be found in [8].

2.3 Numerical strategy

The numerical strategy for the present application is:

- To represent with a discrete forcing method (see Figure 1) (i) the safety valve closing based on an imposed rotated motion, (ii) the air venting valves opening based on the fluid forces, i.e if pressure resulting force is upward oriented,, the position is set to “closed”, if force is downward oriented, it is set to “open” (consequently the possible oscillations are not taken into account);
- To model the complex two-phase flow including free surface, large gas structures or dispersed bubbles with the Generalized Large Interface model from [6,7].

Note that cavitation is neglected by imposing a minimal pressure to 1kPa in the domain and no phase-change.

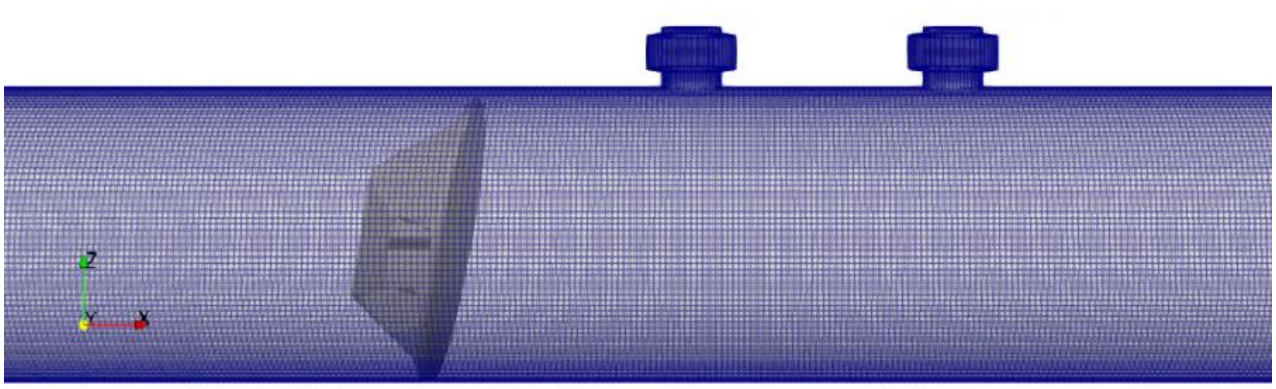

Figure 3 Example of a calculation domain with 2 air-venting valves after the safety valve. Here, valves are represented with the Time and Space Dependent Porosity method.

Prior to the closing valve, a pressure condition is applied in order to have the right pressure in the pipe. The penstock pipe must be long enough to take in account potential air back flows. At the outlet of the pipe, the flow rate is imposed. Outside air-intake valves, an atmospheric pressure condition is applied. A 2nd order URANS model is used for the liquid phase: Rij-SSG and the air phase is considered compressible with a perfect gas assumption.
The time step is adaptative and limited by a maximum CFL condition of 4 for each phase.

A validation from reduced scale to full-scale is proposed. The reduced-scale model description is below.

3. REDUCED-SCALE EXPERIMENT

The aim of these reduced-scale models is to qualitatively reproduce the phenomena which are suspected at the industrial power plant and to provide validation data for the present numerical model. First, the similarity between the full-scale and the reduced-scale experiment for air-water flows is reminded. The geometry and the measured quantities are then described. The selected operating conditions are given and some typical results are presented. Finally, the numerical simulations representing the reduced-scale experiment are discussed.

3.1 Similarity for the air-venting phenomena, choice of a geometric scale and test loop selection

Tests on a scale model are aimed to reproduce the flow around the safety valve during its closing movement and the operation of the vent (opening and air intake). The flow is therefore an air-water two-phase flow.

3.1.1 Similarity and dimensionless numbers

In order to reproduce a similar flow at two different geometric scales, the first condition to fulfill is geometric similarity. The scale factor $\lambda = \frac{L_{model}}{L_{nature}}$ is introduced. The main dimensional numbers for air-water flows, which do not experience any phase change, are (L is a characteristic length, V a characteristic fluid velocity et P is pressure):

- the Froude number, $Fr = \frac{V}{\sqrt{gL}}$, comparing inertia to gravity forces,
- the Reynolds number, $\mathrm{Re} = \frac{VL}{\nu}$, comparing inertia to viscosity forces,

- the Euler number, $Eu = \frac{P_{reference}}{\Delta P_{reference}}$,to account for pressure effects (such as the pressure balance between the atmosphere and the pipe inside),
- the Weber number, $We = \frac{\rho V^2 L}{\sigma}$, comparing inertia to surface tension effects.

These numbers depend on some quantities proportional to the geometric scale, to the operating conditions (velocities and pressures), and on the liquid/gas physical properties (density, viscosity, and surface tension for examples). Note that since in France many hydropower stations are located in mountains, low temperature occurs, and therefore water temperature is assumed around 4°C for the present case. Thus, the vapor pressure is low and vaporization (cavitation) is not expected here, at least during the start of the transient. The vaporization initiated by the pressure decrease is therefore neglected.
In order to reproduce a similar flow at two different scales, we choose to fulfill the Froude similarity. Using the same fluid at both scales, the Reynolds and Weber similarities cannot be fulfilled. The following table gives the corresponding values for a scale ratio around 20 with a penstock diameter of 0.1 m and an inlet velocity of about 1 m/s for the reduced-scale model.

	Operating conditions	Reduced-scale
Froude (-)	1,07	1,07
Reynolds (-)	6 980 399	93 148
Weber (-)	725 128	1 529

Table 1: Dimensionless numbers calculation

3.1.2 Discussion about partial similarity

The Reynolds number is still high enough to ensure turbulent flow at the reduced-scale model. The Weber value is also higher than the critical value of 240 as recommended by the ANSI standard [9] to neglect the surface tension effects. However, the scale ratio around 20, is considered too small to provide enough confidence about quantitative data transposition to real penstock pipes. Therefore, the experimental results are only used to validate CFD results at the reduced scale.

3.1.3 Test loop selection

An already existing test loop is used for the tests, which imposes the range of reachable geometric scales. The MODULAB test loop, located at the EDF Lab Chatou was originally designed as a cavitation test loop, providing an independent control of the flow-rate (through the rotation speed of the circulation pump) and of the pressure level (through the "pressurizer" device, fed by compressed air or by void pump). The following figure gives a sketch and an overall view of the test loop.

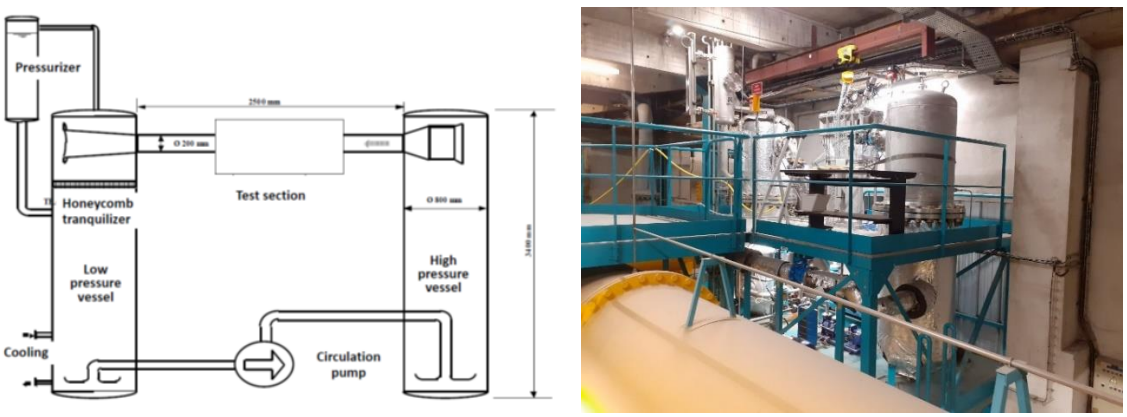

Figure 4 Sketch and overall view of the MODULAB test loop in Chatou

3.1.4 Test section

A dedicated test section was built and inserted between the two reservoirs of the test loop. It represents at reduced-scale the inlet safety valve, the downstream pipe and the vents for the two studied configurations:

- Configuration 1: a single air intake valve right after the safety valve.
- Configuration 2: two air intake valves in the horizontal part, and one larger in the inclined part.

Note that a third configuration, with all vents obstructed, was also tested. The inlet safety valve closure duration is controlled by the operator. The spring stiffness can be varied.

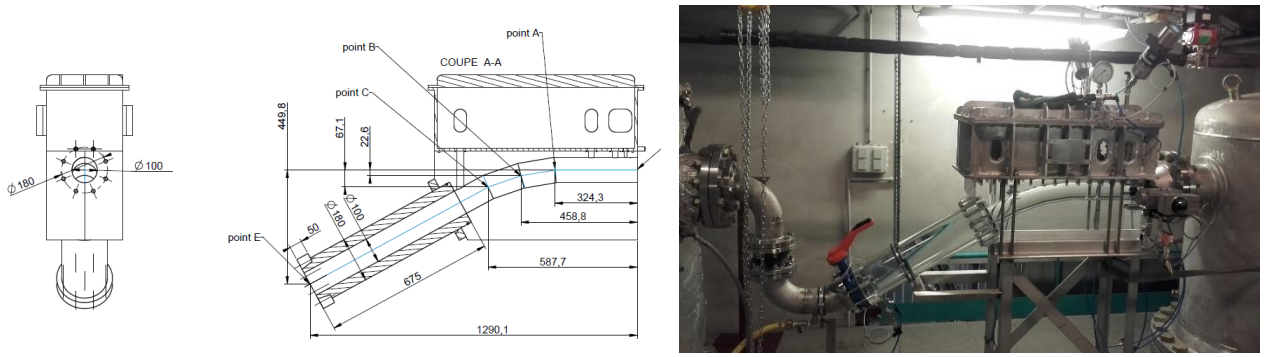

Figure 5 Detailed drawings (left) and view of the test section (right).

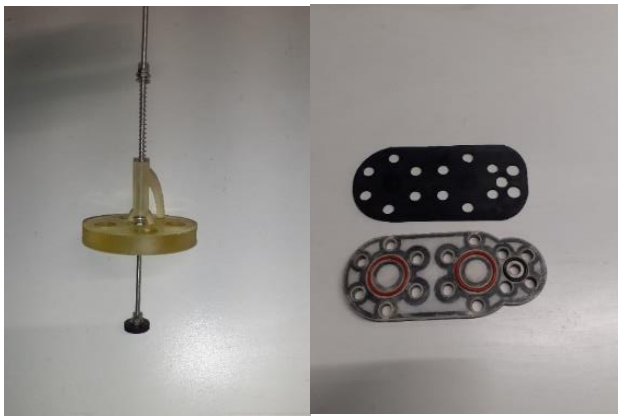

Figure 6 Detailed view of the "configuration 1" air-venting valve.

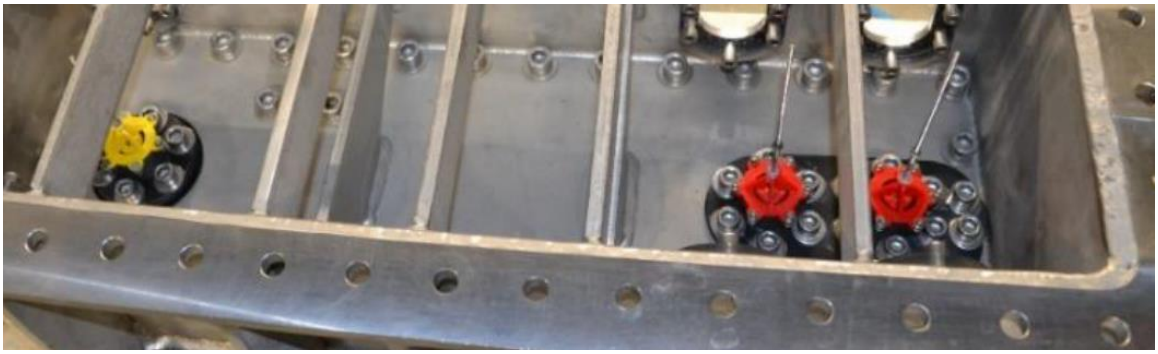

Figure 7 Detailed view of the "configuration 2" air-venting valves

3.2 Instrumentation and tests conditions

The reduced-scale experiment is built transparent, in order to visualize the air-water flow through the vents and inside the pipe, which is the main advantage compared to the nature flow. Videos both of the vent rods (holding the air intake valves) and of the penstock pipe were recorded in a synchronous

way. Moreover, the time evolution of the upstream liquid flow-rate and of several pressures (closed downstream of the safety valve and far downstream) are measured. Note that no air flow-rate has been measured, in order to avoid introducing detrimental head losses for the air entry.
The operating conditions are different flow-rate values for both configurations. Influence of closure duration and of downstream pressure were also tested.

3.3 Experimental results

The reduced-scale experiment succeeded to reproduce the expected phenomena, such as the outflow of water out of the venting valve at the beginning of the inlet safety valve closure, then the air inflow before the inlet safety valve gets fully closed, for the configuration 1. The following figure shows such a flow, with different air structure sizes.

Figure 8 Picture of two-phase air-water flow on the small-scale experiment

The time evolution of the water flow-rate and of the pressure close to the vent are given on the following figure, where the four vertical lines indicate respectively the beginning of the inlet valve closure, the beginning of the vent-rod downward movement (that is its opening), the air entry inside the pipe and the upward movement of the vent-rod.

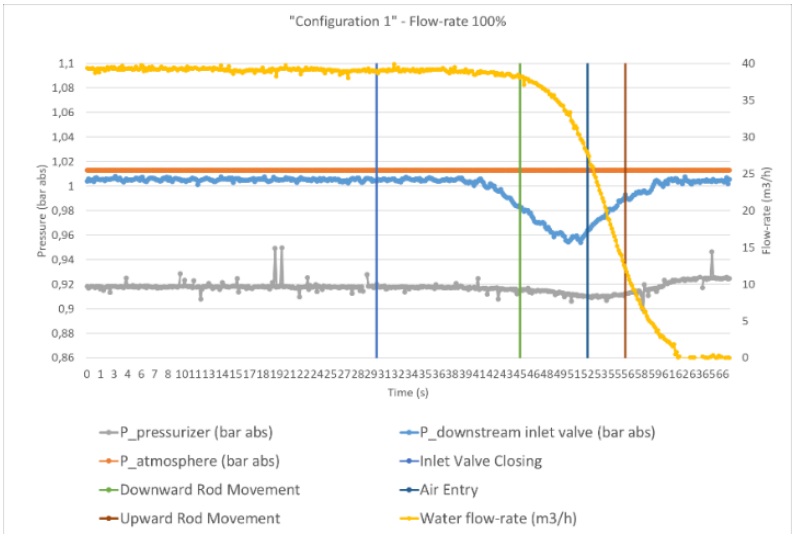

Figure 9 Plot of two-phase air-water flow on the small-scale experiment including pressure evolution, rod motions and water flow rate for configuration 1.

Note that the decreasing water level inside the downstream penstock pipe could not be reproduced at reduced scale, because a closed loop is used which does not allow to empty the downstream reservoir. But this does not qualitatively affect the vent time evolution for the very beginning of the safety valve closure.

The experimental results provided a visual and quantitative behavior of the air vents during the inlet valve closing. The comparative tests confirm lower depressurization of the penstock pipe in configuration 2 compared to configuration 1. They provide qualitative and quantitative data to be used for the code validation at reduced scale.

3.4 Validation of the numerical model

The numerical domain is presented below in Figure 10. It is composed of 3 million hexahedron cells with non-conformal joining for the 4 air-entry pipes.

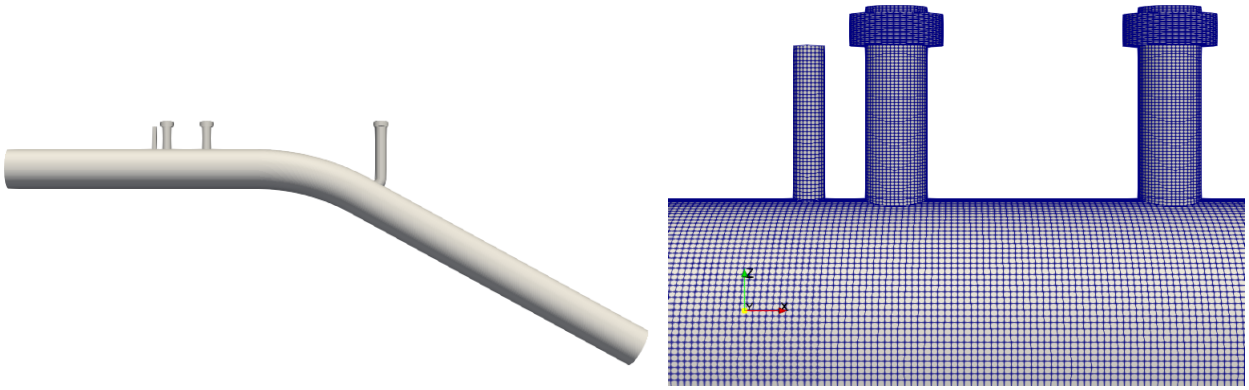

Figure 10 Calculation domain with the different air entries (left) and view of the mesh (right).

Both configurations presented in the experiment description are simulated. Instead of having a pressure condition at the top of the unused air-entry pipes, it is a wall like in the experiment.

With configuration 1 (see Figure 11), the air is going in the reduced-scale penstock pipe from a single air-entry. The air flows through the two first unused pipes (from configuration 2) and some dispersed bubbles are mixing to the main flow whereas larger gas pockets flow at the top of the penstock pipe. With the reduction of the flow rate, large gas structures aggregates until the formation of a free surface connecting the outside and the inside of the reduced-scale penstock pipe.

In configuration 2 (see Figure 12 and 13), there are 3 air-entries, 2 in the horizontal part and 1 in the inclined part. The 2 first ones open quasi simultaneously, the first one ensures a connection between the air outside and inside the pipe, the second one being therefore able to flow a larger amount of air in the existing gas pocket.

The connection between outside and inside is present during the whole scenario after the opening, this free surface counters the pressure decrease inside de penstock pipe. Larger gas structures are present in the second configuration.

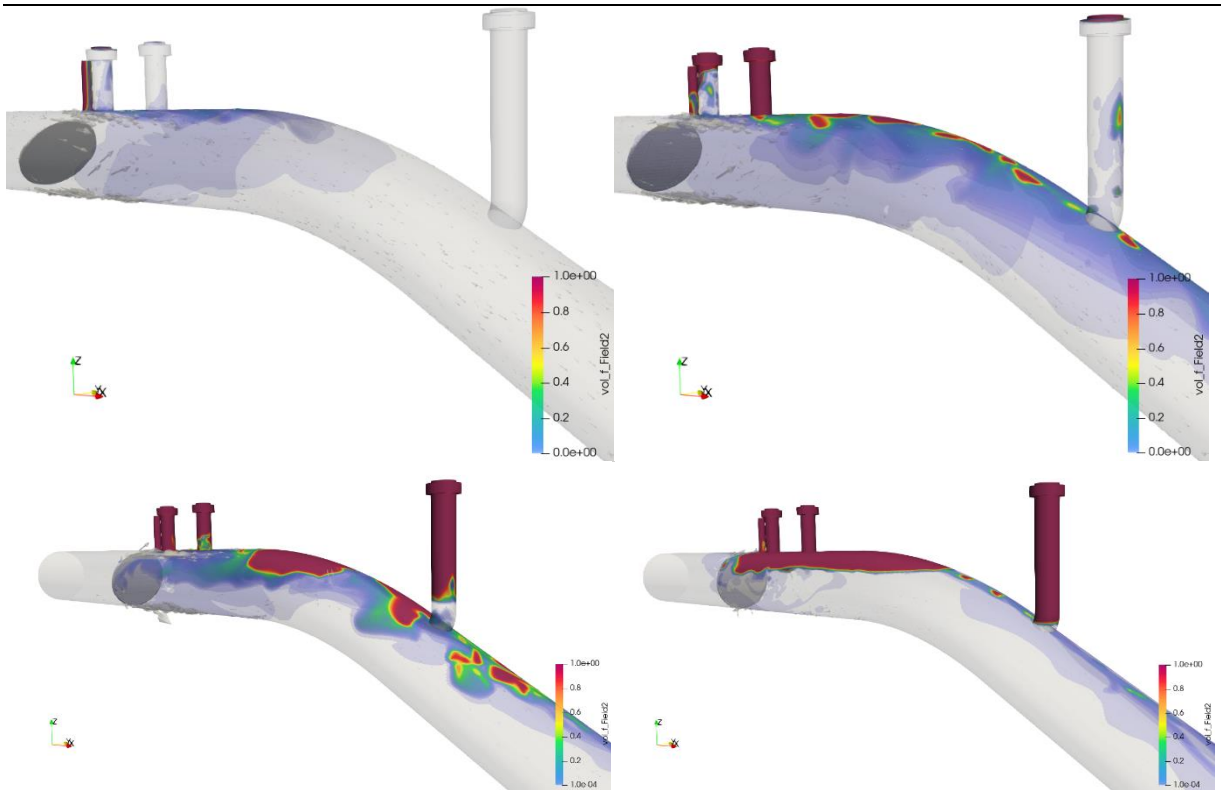

Figure 11 Snapshots of the air-entry in configuration 1 (single air valve). The closing safety valve is in grey. First, air fills the two closed air-pipes of configuration 2. Large gas structures are dropped but there is no free surface created until the reduction of the flow rate due to the closed loop.

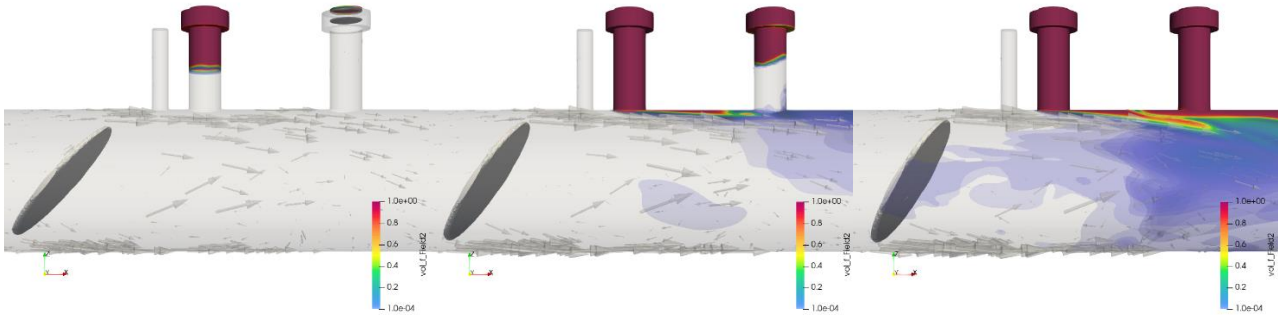

Figure 12 Zoom on the air entry of configuration 2. The closing safety valve is in grey. First, the first air valve opens a large gas structure, then the second air injection is fulfilling the large gas structure.

Regarding the pressure in the vicinity of the closing valve, a satisfactory agreement is found for both configurations on different flow rates (Figure 14 for inlet velocity of 0.75 m/s with configuration 1 and 2). The dynamic of decrease and increase of the pressure is well reproduced as well as the minimum of pressure. A slight discrepancy is noticed in the beginning of the decrease with both configurations, this is due to the not fully constant velocity closing of the valve in the experiment, which is taken constant in the simulation. Regarding the small variations which are present, it depends on the presence of air near the monitoring points which is responsible of these slight variations.

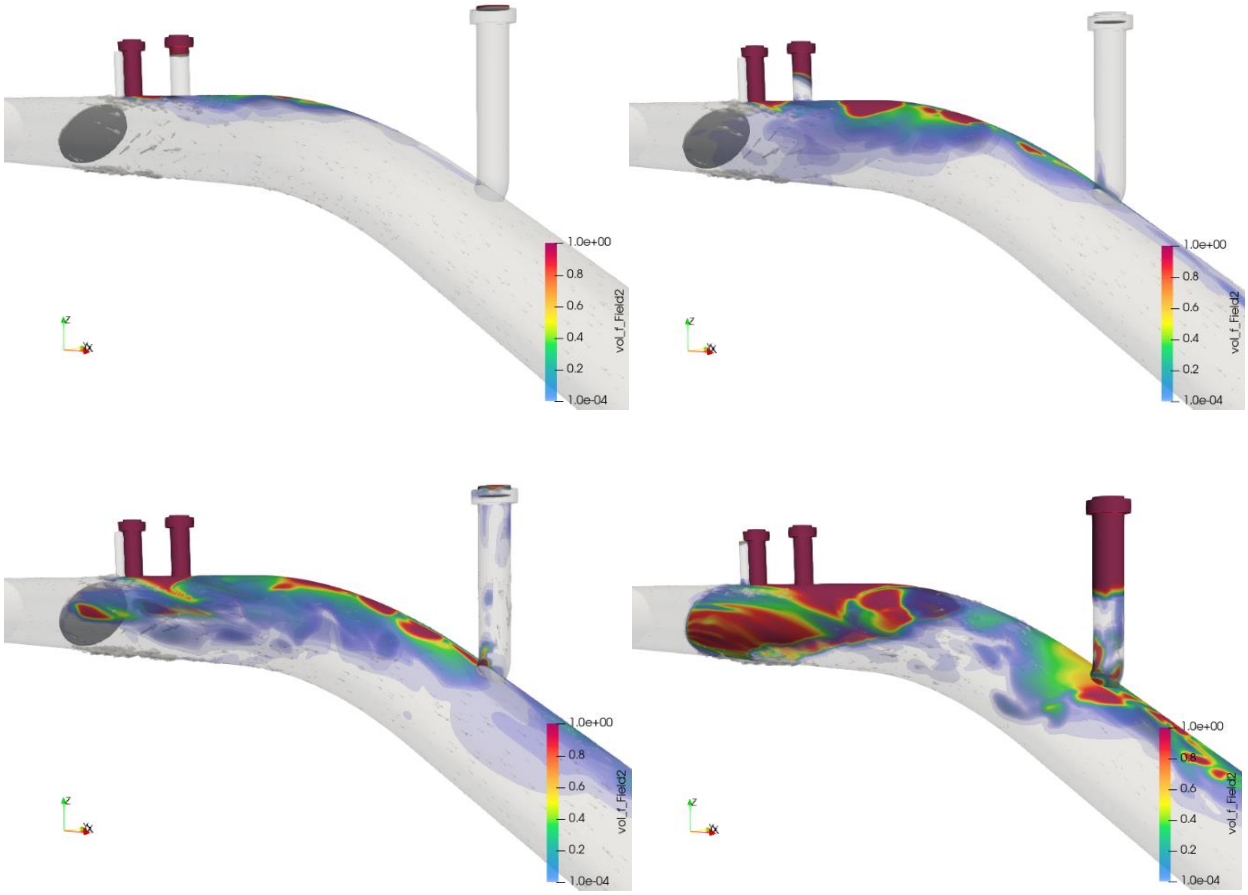

Figure 13 Snapshots of the air-entry in configuration 2 (3 air valves). The closing safety valve is in grey. Large gas structures are present, and there is an air connection between outside/inside the penstock pipe. This large gas structure increases with the decrease of the flow rate.

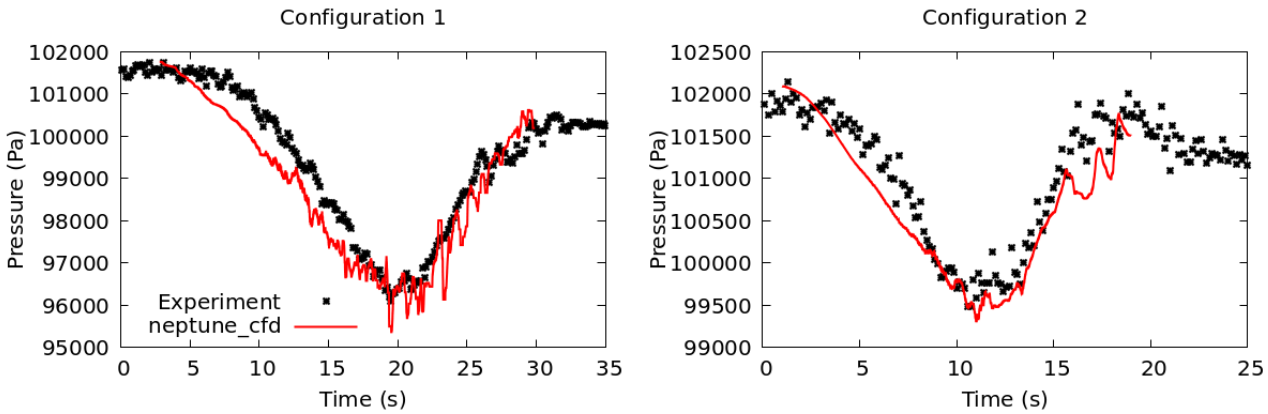

Figure 14 Evolution of pressure in the vicinity of the closing safety valve along time for configuration 1 and 2 in the experiment and from the simulation.

4. AIR ENTRY IN A FULL-SCALE PENSTOCK PIPE

The main discrepancy between the reduced-scale model and real penstock pipes under operating condition remains the water gravitational fall along the length of the penstock pipe which results in a quasi-constant flow-rate along the scenario when measured at the end of the penstock pipe. Thus, when the safety valve is closed, the flow-rate comes from the air intake.
Consequently, the required numerical model to account for gravitational fall has a larger spatial extension since the entrained air might accumulate in the inclined part of the penstock pipe and come back through the horizontal part at the end of the scenario. In order to avoid air loss in the numerical model, a longer inclined part is considered based on an extrusion of the model. A single air venting valve is present in the vicinity of the safety valve. The present calculation domain is composed of 5.7 million of hexahedron cells.
For the present case, model is validated against data coming from operating condition measurements. The safety valve closure is imposed based on real operating conditions, as well as the inlet pressure or the flow rate at the end of the penstock pipe.

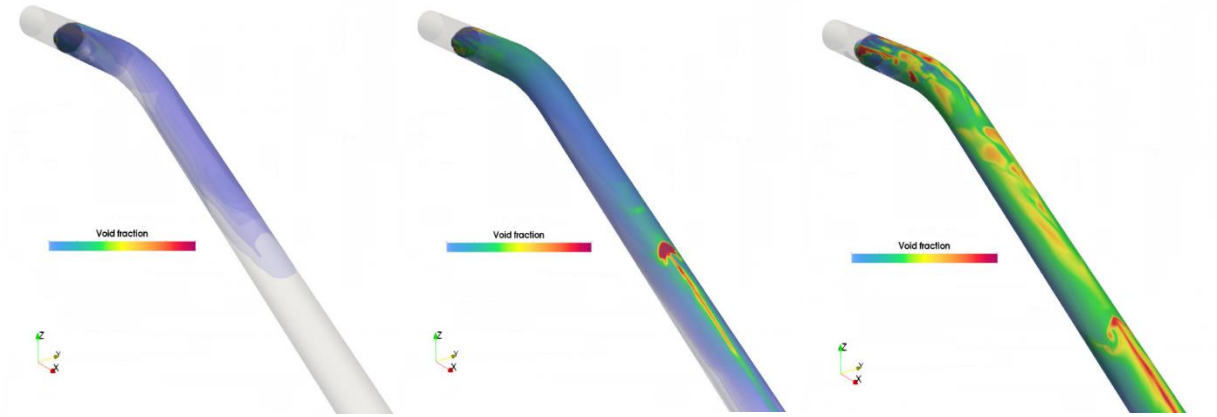

Figure 15 Numerical predictions of air venting inside the penstock pipe for different instants of the scenario.

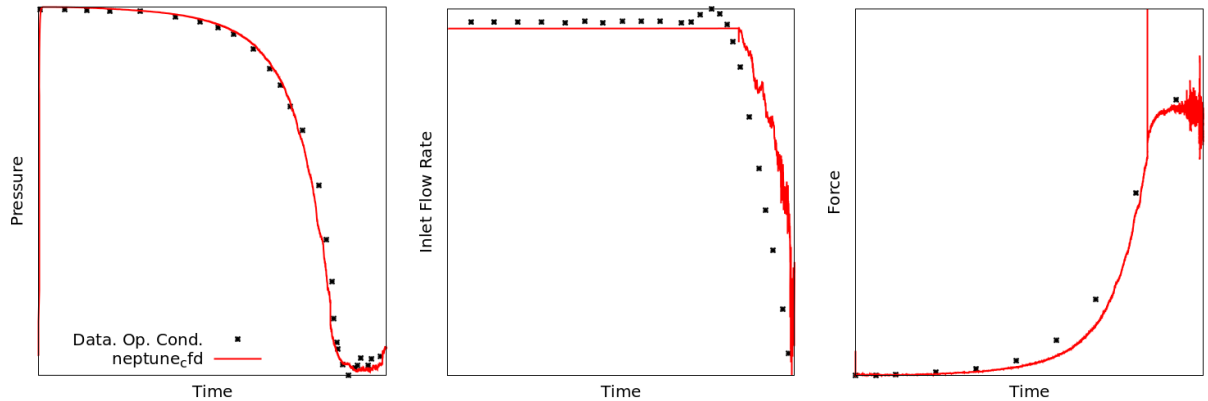

Figure 16 Numerical results on the pressure after the safety valve compared to measurements, inlet flow rate and force acting on the safety valve compared to safety valve manufacturer data.

Figure 15, it is possible to see similar behavior with the reduced-scale simulations; however, in comparison the bubble diameter being smaller regarding the penstock pipe diameter, there is air in the whole domain with a very small diameter and some large gas structures following the air intake valve and in the inclined part (this is due to the non-respect of Weber similarity in the reduced-scale model).
Figure 16, the pressure is well predicted by the numerical model compared to the measurements at full-scale. The decrease of the pressure and its evolution during the air intake are in satisfactory

agreement. Moreover, numerically, the air intake valve opens precisely when the force acting on it flips like in the scenario (at the same time). The slight pressure underestimation in the venting part is probably due a to slight overestimation of the inlet flow rate (which is a result of simulation since a pressure condition is imposed at the inlet). Nevertheless, the prediction of the force acting at the valve is also in good agreement with the prediction from the manufacturer. The present results show the ability of the numerical model to predict such scenario with a satisfactory agreement.

5. CONCLUSIONS

A two-phase numerical model able to take into account the motion of safety valve and air venting valve is presented. It is based on a Eulerian-Eulerian CFD code, called neptune_cfd, with a multi-regime approach (combining dispersed and continuous gas phase models), and on a discrete forcing method, called Time and Space Dependent Porosity method, to track structure motions.

A reduced-scale experiment is presented in order to validate the CFD model. A Froude similarity is used to define the characteristics of the model. Two configurations are possible, one with a single air venting valve, and another with three venting valves. Pressures, vane motion and the flow rate (in the closed loop) are recorded along time for different scenarii.

The numerical model is then validated on reduced-scale and full-scale based on pressure evolution. A satisfactory agreement is observed for the two scales meaning that the numerical model is able to predict the air intake correctly and its effect on pressure evolution inside the penstock pipe.

This kind of tool, based on CFD, presents real advantages to design air intake systems in penstock pipes or to evaluate existing ones. It needs a complete validation, and a phase change model to tackle the worst scenario when it might occur.

ACKNOWLEDGEMENTS

The authors would like to thank Vincent Lhuillier, Vinicius Alves Fernandes, Jean-Louis Toribio, David Graveleine, Cedric Bernardi, Philippe Fanouillère and Joris Dupret for their help and advice in the present work.

REFERENCES

[1] Falwey Henry T., Air-water flow in hydraulic structures, US Dpt of Interior, 1980.

[2] Sadeque F., Charrette H., Z Shawwash Z., An investigation of air inflow into hydropower conduits during emergency closure, “Pressure Surges” congress, Bordeaux, France, November 2018.

[3] Guelfi, A, Bestion, D, Boucker, M, Boudier, M, Fillion, P, Grandotto, M, Hérard, J-M, Hervieu, E, and Peturaud, P (2007). “NEPTUNE: A New Software Platform for Advanced Nuclear Thermal Hydraulics,” *Nucl Sci Eng*, 15(3), 281–324. https://doi.org/10.13182/NSE05-98.

[4] Ishii, M (1975). Thermo-fluid Dynamic Theory of Two-phase Flow, Eyrolles, 248 pp.

[5] Coste, P (2013). “A Large Interface Model for Two-phase CFD,” *Nucl Eng Des*, 255, 38–50. https://doi.org/10.1016/j.nucengdes.2012.10.008.

[6] N. Mérigoux, Multiphase Eulerian-Eulerian CFD supporting the nuclear safety demonstration, Nuclear Engineering and Design, Volume 397, 2022, 111914, ISSN 0029-5493, https://doi.org/10.1016/j.nucengdes.2022.111914.

[7] Mer, S, Praud, O, Neau, H, Merigoux, N, Magnaudet, J, and Roig, V (2018). "The Emptying of a Bottle as a Test Case for Assessing Interfacial Momentum Exchange Models for Euler–Euler Simulations of Multi-scale Gas-liquid Flows," *Int J Multiphase Flow*, 106, 109–124. https://doi.org/10.1016/j.ijmultiphaseflow.2018.05.002.

[8] Benguigui, W, Doradoux, A, Lavieville, J, Mimouni, S, and Longatte, E (2018). "A Discrete Forcing Method Dedicated to Moving Bodies in Two-phase Flows," *Int J Numer Methods Fluids*, 88(7), 315–333. https://doi.org/10.1002/fld.4670.

[9] American National Standards for Rotodynamic Pumps for Pump Intake Design, ANSI/HI 9.8-2012, December 2012.